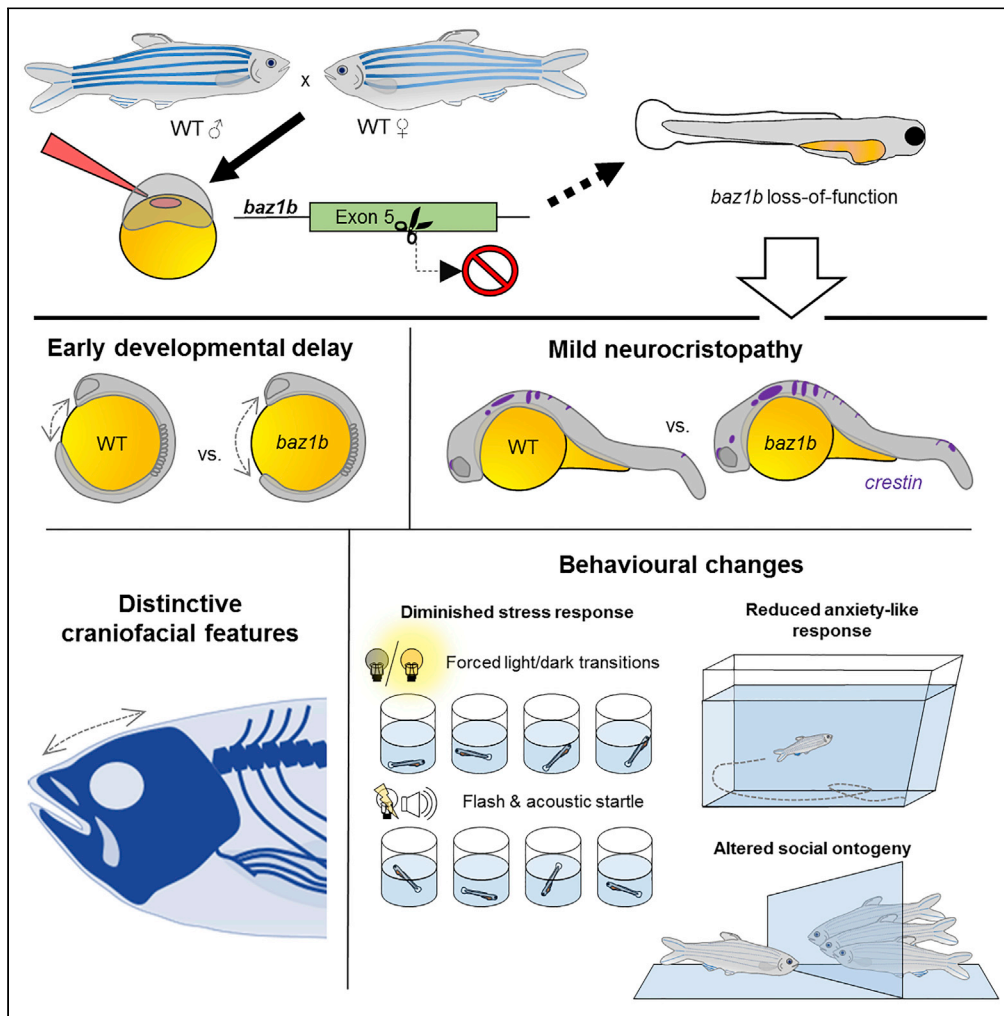


Article

baz1b loss-of-function in zebrafish produces phenotypic alterations consistent with the domestication syndrome



Jose V. Torres-Pérez, Sofia Anagianni, Aleksandra M. Mech, ..., Scott E. Fraser, Giorgio Vallortigara, Caroline H. Brennan

jose.vicente.torres@uv.es (J.V.T.-P.)
c.h.brennan@qmul.ac.uk (C.H.B.)

Highlights
In zebrafish, *baz1b* regulates neural crest development and craniofacial features

Developmental deficits in *baz1b* result in reduced anxiety-associated phenotypes

Developmental deficits in *baz1b* alter the ontogeny of social behaviors in zebrafish

baz1b regulates phenotypes associated with the domestication syndrome

Torres-Pérez et al., iScience
26, 105704
January 20, 2023 © 2022 The Authors.
<https://doi.org/10.1016/j.isci.2022.105704>



Article

baz1b loss-of-function in zebrafish produces phenotypic alterations consistent with the domestication syndrome

Jose V. Torres-Pérez,^{1,2,*} Sofia Anagianni,¹ Aleksandra M. Mech,^{1,6} William Havelange,^{1,6} Judit García-González,^{1,3} Scott E. Fraser,⁴ Giorgio Vallortigara,⁵ and Caroline H. Brennan^{1,7,*}

SUMMARY

BAZ1B is a ubiquitously expressed nuclear protein with roles in chromatin remodeling, DNA replication and repair, and transcription. Reduced BAZ1B expression disrupts neuronal and neural crest development. Variation in the activity of BAZ1B has been proposed to underly morphological and behavioral aspects of domestication through disruption of neural crest development. Knockdown of *baz1b* in *Xenopus* embryos and *Baz1b* loss-of-function (LoF) in mice leads to craniofacial defects consistent with this hypothesis. We generated *baz1b* LoF zebrafish using CRISPR/Cas9 gene editing to test the hypothesis that *baz1b* regulates behavioral phenotypes associated with domestication in addition to craniofacial features. Zebrafish with *baz1b* LoF show mild underdevelopment at larval stages and distinctive craniofacial features later in life. Mutant zebrafish show reduced anxiety-associated phenotypes and an altered ontogeny of social behaviors. Thus, in zebrafish, developmental deficits in *baz1b* recapitulate both morphological and behavioral phenotypes associated with the domestication syndrome in other species.

INTRODUCTION

Bromodomain adjacent to zinc finger domain 1B (BAZ1B), also known as Williams syndrome transcription factor, is a member of the BAZ family of bromodomain proteins with roles in chromatin remodeling, DNA replication and repair, and transcription. It also possesses atypical kinase activity.¹ BAZ1B is one of 28 genes in the 7q11.23 region that is disrupted in Williams syndrome (WS, or Williams-Beuren Syndrome), a neurodevelopmental condition associated with craniofacial dimorphisms and cognitive and behavioral traits including pro-social behavior.^{2,3} In contrast, in Williams XY Syndrome, haplo-duplication of this chromosomal region leads to autism-like disorders.^{4,5} Similarities between WS-associated craniofacial features and those of domesticated species when compared to their wild-type counterparts, and the observation that *baz1b* expression correlates with domestication in canids, has led to the suggestion that variants in *baz1b* may play a central role in domestication.^{6–8}

In humans, BAZ1B is expressed in adult heart, brain, placenta, skeletal muscle, and ovary, and in brain, lung, kidney, and liver at fetal stages.⁹ In *Xenopus laevis*, *baz1b* is ubiquitously expressed until early neurulation, when its expression gets restricted to the neural ectoderm and neural tube.¹⁰ At later stages, *baz1b* localizes to the neural tube, optic cup, anterior brain, migrating cranial neural crest cells, and the branchial (pharyngeal) arches.¹⁰

The haploinsufficiency of BAZ1B disrupts gene expression in neural stem cells.¹¹ Similarly, morpholino knockdown of *baz1b* expression in *Xenopus* embryos leads to altered expression of several genes, many of which play important roles during development (e.g. *BMP4*, *Shh*, *pax2*, *mrf4*, *sox2*, *epha4*, and *NCAM*). Developmental processes regulated by these gene products include the balance between neural and non-neural tissue formation, mesoderm and neuronal patterning and differentiation, the balance between proliferative and non-proliferative cells, neural crest differentiation and migration, and axonal pathfinding and dendritic spine formation.¹² Morphant *Xenopus* embryos gastrulate normally but show reduced anterior posterior body length, abnormal axis curvature, reduced neural tissue, and abnormal craniofacial development.

¹School of Biological and Behavioural Sciences, Queen Mary University of London, London E1 4NS, UK

²Departament de Biologia Cel·lular, Biologia Funcional i Antropologia física, Fac. de CC. Biològiques, Universitat de València, C/ Dr. Moliner 50, Burjassot, València 46100, Spain

³Department of Genetics and Genomic Sciences, Icahn School of Medicine, Mount Sinai, New York, NY 10029, USA

⁴Michelson Center for Convergent Bioscience, University of Southern California, Los Angeles, CA, USA

⁵Center for Mind/Brain Sciences, University of Trento, Rovereto, Italy

⁶These authors contributed equally

⁷Lead contact

*Correspondence: jose.vicente.torres@uv.es (J.V.T.-P.), c.h.brennan@qmul.ac.uk (C.H.B.)

<https://doi.org/10.1016/j.isci.2022.105704>



In addition to effects on early patterning and neural development, in both neural crest stem cells *in vitro* and *Xenopus* embryos, *baz1b* regulates the balance between neural crest cell precursors and migratory cells. Differential gene expression analysis of *BAZ1B* dosage effects in 32 independent neural crest stem cell lines highlighted disruption of key neural crest-specific transcriptional circuits, including a regulatory axis involved in neural crest-mediated craniofacial morphogenesis.⁶ The effect of *BAZ1B* knockdown varied depending on the line, thus suggesting the genetic background influences transcriptional vulnerability to variations in *BAZ1B* dosage.⁶ In *Xenopus* embryos, knockdown of *baz1b* leads to delayed migration of neural crest, apoptosis, and consequent disruption of neural crest-derived skeletal components such as craniofacial bones.¹² Craniofacial features including protruding forehead and shorter snout are also seen in *Baz1b* LoF mice¹³ and are similar to craniofacial features seen in patients with WS.¹ These craniofacial features associated with *Baz1b* knockdown show similarity to those seen in domesticated species when compared to their wild counterparts. Similarly, paleogenomic analysis also points to a role for *BAZ1B* in the evolution toward reduced facial features in modern humans.⁶

The craniofacial features associated with domestication in animals are also associated with behavioral changes including increased sociability, lower aggressiveness, and reduced fear- and stress-related behaviors.^{14,15} According to the neural crest domestication hypothesis (NCDS), mild neural crest deficits result in less/slower input of cells to the target structures, which ultimately accounts for not only reduced craniofacial features but also hypofunction of adrenal and sympathetic ganglia, extended the immaturity period of the hypothalamus-pituitary-adrenal (HPA) axis, and significantly reduced size in certain components of the forebrain's limbic system.¹⁶ Mild neurocristopathy is also associated with an extended immaturity period that supports the existence of a longer "socialization window" during early life.^{16–18} Therefore, the NCDS hypothesis offers a unitary explanation for all the DS-traits with a predicted genetic component involving the development of the neural crest. In agreement with this hypothesis, variants in neural crest development regulatory genes are associated with domestication with *BAZ1B* being recently suggested as a key regulator of this process.⁶ However, due to the plethora of processes in which the neural crest is involved, it is likely that selective pressure toward pro-social behavior selected for variants in neural crest development without such variants necessarily being causal.¹⁸ Thus, here we directly test the hypothesis that *baz1b* regulates both morphological and pro-social behavioral phenotypes associated with domestication using zebrafish (*Danio rerio*) as a model species.

Zebrafish have emerged as a novel organism in which to assess different aspects of behavioral neuroscience. The relative ease of generating genetic mutants, the conserved neuronal circuitry,¹⁹ and the fact that around 80% of genes associated with human diseases have a corresponding ortholog²⁰ make zebrafish an ideal model in which to study the genetics and neuronal circuitry underlying behavior. Zebrafish can be of use to identify the effect of individual genes which are part of a genomic region with high linkage disequilibrium, such as *baz1b* in WS.

Our research shows that zebrafish *baz1b* LoF mutants show mild underdevelopment of the neural crest at larval stages, and distinctive craniofacial features and reduced anxiety-associated phenotypes later in life. During the ontogeny of social behavior, *baz1b* LoF mutants show an increased inclination to interact with conspecifics. Similar changes in facial morphology and behavior are associated with domestication of animals and in human evolution. Thus, morphological and behavioral phenotypes seen in *baz1b* LoF zebrafish support delayed neural crest development as a mechanism underlying domestication and a key role of *baz1b* in this process.

RESULTS

CRISPR/Cas9 induction of stable *baz1b* LoF zebrafish lines

We used the CRISPR/Cas9 system to induce mutations in the zebrafish *baz1b* gene. Two lines were established, one, *baz1b*^{del44}, carrying a 44-base pair (bp) deletion at exon 5, and the other, *baz1b*^{ins35}, with a 35 bp insertion at exon 5. Both mutations result in the introduction of a premature stop codon (Figures 1A and S1A). Quantification of *baz1b* mRNA levels by qPCR (Figures 1B and S1B) revealed a significant difference in expression between genotypes in both lines (*baz1b*^{del44}: F (2, 6) = 7.415, p = 0.024; *baz1b*^{ins35}: F (2, 6) = 21.97, p = 0.002). Post-hoc analysis of the *baz1b*^{del44} line showed that both heterozygous (HET, p = 0.042) and homozygous (HOM, p = 0.032) fish had significantly lower expression of *baz1b* than wild-type (WT) siblings, while there was no significant difference between HET and HOM (p = 0.973). On the *baz1b*^{ins35} line, post-hoc analysis showed that HOM had significantly lower expression than WT (p = 0.001) while HET failed to reach significance (vs. WT: p = 0.064; vs. HOM: p = 0.023).

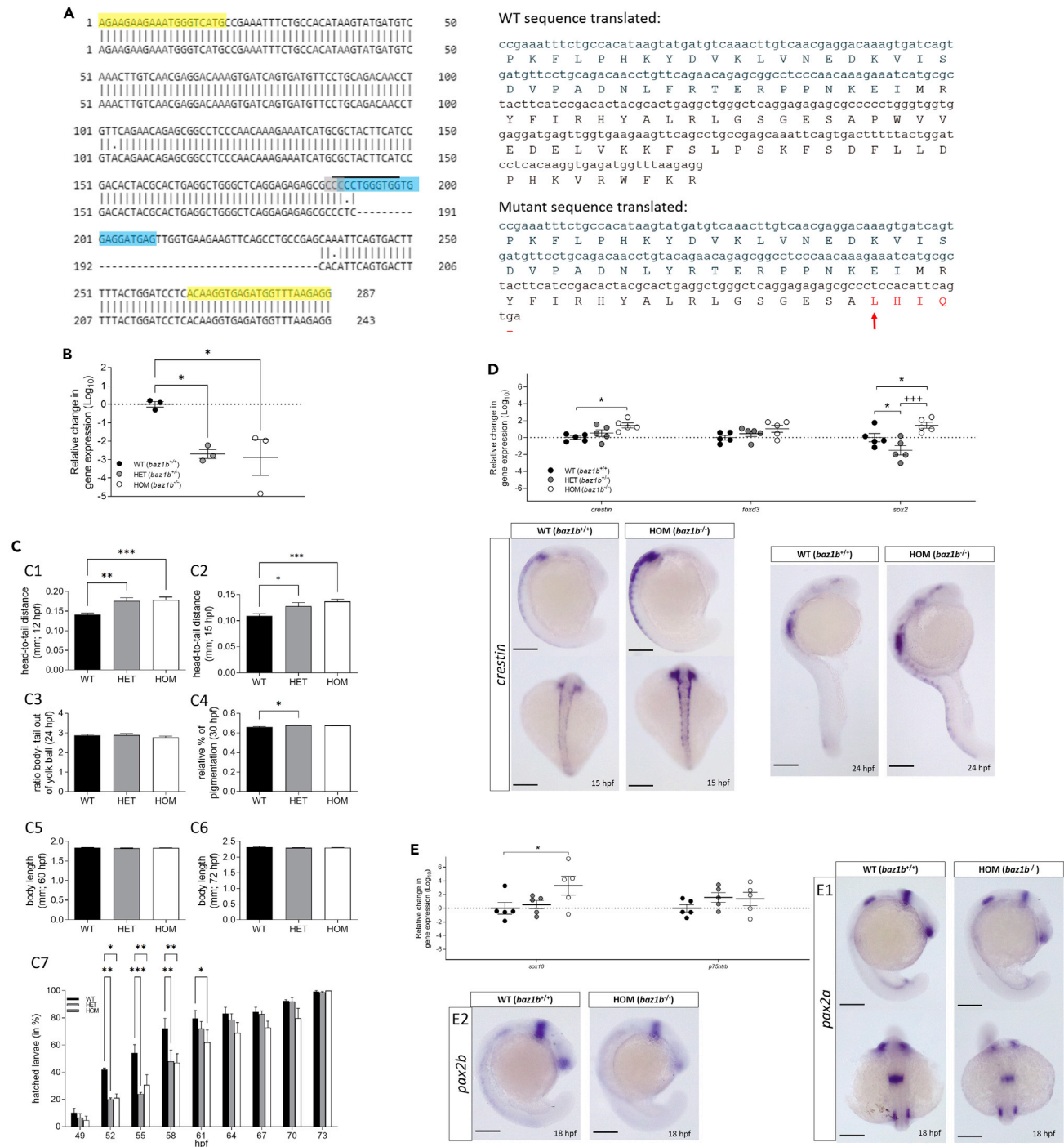


Figure 1. Deficits in *baz1b* lead to mild neurocristopathy in zebrafish

(A) Left panel shows a DNA blast for the portion of *baz1b*'s exon 5 amplified by PCR used for genotyping between WT (above) and mutants (below, 44 bp deletion). Primers used are highlighted in yellow, crRNA site in blue, PAM site in gray and restriction enzyme over-lined. Right panel shows the in-frame translation to amino acids (aa) sequences in WT (above) and mutants (below) of the same exon 5 portion. Arrow indicates mutation starting site, changed aa are in red and stop codon marked as a dash (–).

(B) Relative change in gene expression (\log_{10}) assessed by qPCR between 5 dpf larvae from each genotype showing that in both HET and HOM the expression of *baz1b* is significantly diminished with respect to WT. Figure shows individual values ($N = 3$ per genotype, each representing a group of 16 larvae combined) and mean \pm SE mean (SEM).

Figure 1. Continued

(C) Developmental comparison between the three phenotypes for the head-to-tail distance at 12 hpf (C1) and at 15 hpf (C2), ratio body/tail-out-of-yolk-ball at 24 hpf (C3), relative percentage of pigmentation at 30 hpf (C4), body length at 60 hpf (C5) and at 72 hpf (C6), and percentage of hatched larvae between 49 and 73 hpf (C7).

(D) Relative change in gene expression (\log_{10}) for *crestin*, *foxd3*, and *sox2* from each genotype at 24 hpf. Below panel shows whole larvae *in situ* hybridization (WISH) against *crestin* for WT and HOM at 18 and 24 hpf.

(E) Relative change in gene expression (\log_{10}) for *sox10* and *p75ntrb* from each genotype at 24 hpf with WISH against *pax2a* (E1) and *pax2b* (E2), genes regulated by *baz1b*. Graphs show mean \pm SEM. In all cases: * $p < 0.05$; ** $p < 0.01$; *** $p < 0.001$; **** $p < 0.001$. Statistical test: one-way ANOVA with Tukey correction for multiple comparison for B, C2, C4, C5, D, and E; non-parametric test of Kruskal-Wallis corrected for multiple comparison for C1, C3, and C6; two-way ANOVA with repeated measures with Tukey correction for multiple comparison for C7. Scale bars represent 200 μm .

Since the primers target a region of the mRNA upstream from the mutation site, the decrease in functional mRNA suggests that the mRNA surveillance pathway interpreted the premature stop codon as aberrant and targeted the mRNA for degradation,²¹ consistent with establishment of a LoF line. As *baz1b^{del44}* showed the most significant reduction in mRNA, we have focused on analysis of this line. However, *baz1b^{ins35}* showed similar morphological and behavioral differences as reported in supplementary figures (Figures S1, S3–S5, and S7).

***baz1b* LoF leads to mild developmental delay at early stages**

The expression of *baz1b* begins during gastrulation²² and *baz1b* knockdown in *Xenopus* leads to shortened body axis and disrupted morphology at larval stages.¹² Thus, we examined the impact of *baz1b* LoF on zebrafish development by assessing multiple morphological characteristics at different developmental points (Figure 1C). At 12 h post fertilization (hpf), there was a significant difference in the head-to-tail distance between genotypes (H (2) = 16.45, $p < 0.001$), with both HET ($p = 0.002$) and HOM ($p = 0.001$) embryos showing significantly larger distances than WT, suggesting delayed development. Similar differences were observed at 15 hpf (F (2, 78) = 7.480, $p = 0.001$; HET vs. WT: $p = 0.047$; HOM vs. WT: $p = 0.001$).

Analyses at 24 or 60 hpf found no significant differences in overall body length (Figure 1C). Nonetheless, a significant difference in the relative percentage of pigmentation was observed between genotypes at 30 hpf (F (2, 42) = 3.840, $p = 0.029$; Figure 1C4) with post-hoc comparison describing a marginally significant increase in HET ($p = 0.045$) vs. WT. No other pairwise comparisons were significant. Additionally, analysis of hatching rate showed a significant interaction between time and genotype (F (16, 48) = 3.292, $p = 0.001$; Figure 1C7). Post-hoc pairwise comparison revealed that the percentage of hatching was higher in WT than mutant siblings between 52 and 61 hpf (52 hpf: WT, vs. HOM: $p = 0.011$, vs. HET: $p = 0.007$; 55 hpf: WT, vs. HOM: $p = 0.004$, vs. HET: $p < 0.001$; 58 hpf: WT, vs. HOM: $p = 0.002$, vs. HET: $p = 0.002$; 61 hpf: WT, vs. HOM: $p = 0.035$) but did not differ at later time points.

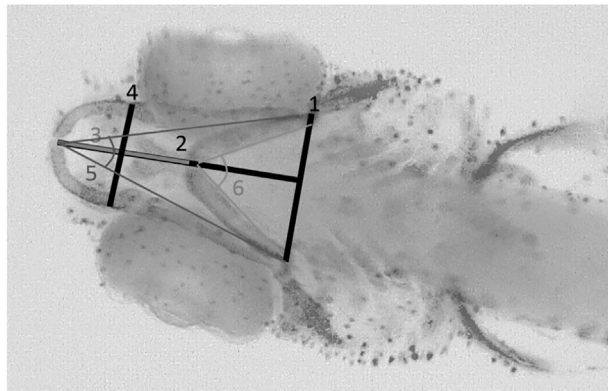
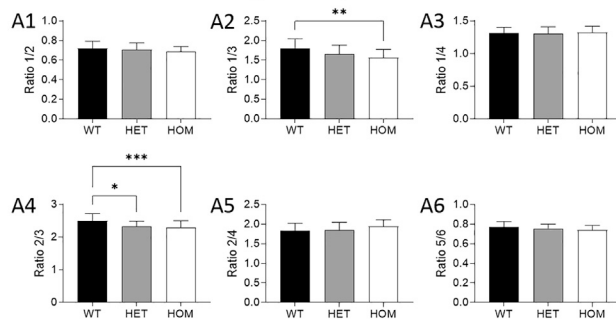
Changes with a similar directionality were observed in the *baz1b^{ins35}* (Figure S1).

***baz1b* LoF zebrafish show mild neurocristopathy**

As *Baz1b* knockdown has been suggested to lead to a delay in neural crest development, we examined the expression of key genes within the neural crest development pathway (*sox2*, *sox10*, *crestin*, *foxd3*, and *p75ntrb*) by qPCR, and the pattern of expression of *sox10*, *foxd3*, and *crestin* as well as other genes shown previously to be affected by *baz1b* knockdown (*pax2a*, *pax2b*, and *epha4^{12,23–26}*) by *in situ* hybridization. The analysis by qPCR of markers of neural crest development showed increased expression of *crestin* in HOMs compared to WT siblings ($p = 0.034$; Figure 1D), increased expression of *sox10* in HOMs ($p = 0.044$; Figure 1E), and decreased expression of *sox2* in HETs ($p = 0.028$; Figure 1D) but increased expression in HOMs ($p = 0.0318$; HET vs. HOM: $p < 0.001$). There were no differences in *foxd3* or *p75ntrb* expression (Figures 1D and 1E, respectively). The increased level of expression of *crestin* was evident on whole-body *in situ* hybridization (WISH) analysis of larvae at all developmental stages examined (Figure 1D). No differences in expression of *sox10* or *foxd3* were seen on WISH analysis but reduced expression of *epha4*, *pax2a*, and *pax2b* was seen in homozygous mutants compared to controls. (Figures 1E and S2). The reduced expression of *pax2a/b* and *epha4* was most evident in anterior areas, including the hind-brain and the optic vesicles.

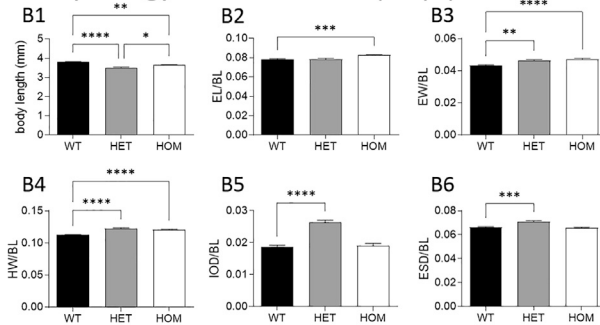
Similarly, the other zebrafish line, *baz1b^{ins35}*, HETs showed a significant increase in *crestin* when compared to WT, while HOMs showed a reduction in *foxd3* (Figure S1).

A Alcian blue staining at 5 dpf



1: width of the ceratohyal (CH) at palatoquadrate (PQ) joint; 2: length 1 to Meckel's cartilage (M); 3: length M-CH; 4: width M at PQ joint; 5: M-PQ angle; 6: CH angle

B Morphology of intact larvae (5 dpf)



C Morphology of intact juveniles (30 dpf)

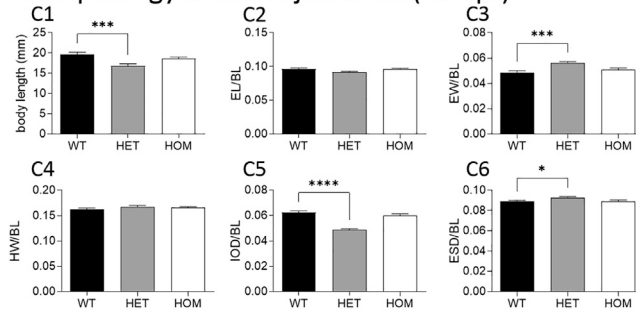


Figure 2. *baz1b* LoF zebrafish have altered craniofacial features

(A) Comparison between genotypes for the cranial features (outlined in the picture below) observed at 5 dpf by Alcian blue staining: ratio 1/2 (A1), ratio 1/3 (A2), ratio 1/4 (A3), ratio 2/3 (A4), ratio 2/4 (A5), and ratio 5/6 (A6).
 (B) Morphological comparisons of intact 5 dpf for the three genotypes: body length (BL, in mm; B1), eye length (EL) normalized to BL (B2), eye width (EW) normalized to BL (B3), head width (HW) normalized to BL (B4), inter-ocular distance (IOD) normalized to BL (B5), and eye-snout distance (ESD) normalized to BL (B6).
 (C) Morphological comparison of intact juvenile fish (30 dpf). Graphs show mean \pm SEM. In all cases: * $p < 0.05$; ** $p < 0.01$; *** $p = 0.001$; **** $p < 0.001$. Statistical test: one-way ANOVA with Tukey correction for multiple comparison for A1, A3, A5, A6, B2–B6, and C1–C6; non-parametric test of Kruskal-Wallis corrected for multiple comparison for A2, A4, and B1.

***baz1b* LoF zebrafish have altered craniofacial features**

Given the role of neural crest in craniofacial development and the suggested role of *baz1b* in this process,^{6,12,13} we investigated whether *baz1b* LoF induced craniofacial differences in zebrafish.

Larvae of 5 dpf from all genotypes were stained with alcian blue to measure their bone structures (Figure 2A). Statistical analysis revealed that the ratio |width of the ceratohyal (CH) bone: length from Meckel's cartilage (M) to CH|, a measure used in previous published works assessing craniofacial development in zebrafish,^{27–29} was statistically different ($H(3) = 12.53, p = 0.002$). Multiple pairwise post-hoc comparison revealed this to be driven by a decrease in HOM ($p = 0.002$) when compared to WT siblings. Additionally, the ratio |length of M: length from M to CH| was also significantly different ($H(3) = 14.87, p = 0.001$) with multiple pairwise post-hoc comparisons showing a reduction in both HET ($p = 0.039$) and HOM ($p = 0.001$) compared to WT. No other comparisons were significantly different.

To confirm that the changes in cranial bones were leading to facial variations (affecting the final shape of the soft tissues above the bones), we also performed morphological analysis of whole unstained larvae at 5 dpf (Figure 2B). Firstly, we observed a significant difference in total body length (BL) between genotypes ($H(3) = 39.12, p < 0.001$) with both HET and HOM showing reduced BL compared to WT siblings (HET: $p < 0.001$, HOM: $p = 0.002$). Reduction in BL was more pronounced in HET (HET vs. HOM: $p = 0.013$). Thus, the analysis of the additional partial body measurements (below) was done after standardizing by BL.

We observed a significant change in eye length (EL, $F(2, 57) = 9.465, p < 0.001$) and eye width (EW, $F(2, 57) = 12.54, p < 0.001$) between genotypes, which post-hoc analysis showed to be driven by HOM having an increase for both (EL: $p = 0.0009$; EW: $p < 0.001$) and HET only for EW ($p = 0.001$) when compared to WT. Additionally, total head width (HW) was found to be significantly different between genotypes ($F(2, 57) = 35.05, p < 0.001$) with both HET ($p < 0.001$) and HOM ($p < 0.001$) showing a significant increase when compared to WT. Furthermore, a significant difference was also observed regarding the inter-ocular distance (IOD, $F(2, 57) = 40.35, p < 0.001$) and the eye-snout distance (ESD: $F(2, 57) = 14.36, p < 0.001$), which in both cases post-hoc analysis revealed to be driven by a significant increase in the HET compared to WT (IOD: $p < 0.0001$; ESD: $p = 0.001$).

At 30 dpf, fish were assessed on their maturation scores.³⁰ These maturation scores rely on four external morphological characteristics (pigment pattern, tail fin, anal fin, and dorsal fin morphology) to determine their larval stage. No significant difference in the maturation scores was observed between the three genotypes ($F(2, 57) = 1.013, p = 0.370$; mode in all genotypes was 4). In addition to assessing maturation, we analyzed corresponding craniofacial measurements at 30 dpf, similarly as done at 5 dpf, to assess if changes were maintained at later stages (Figure 2C). There was a significant difference in BL ($F(2, 57) = 9.538, p < 0.001$) and post-hoc comparison revealed it to be driven by a reduction in HET ($p < 0.001$) when compared to WT. Significant differences in EW were observed by genotype ($F(2, 57) = 9.084, p < 0.001$) with HET showing significantly wider eyes than WT ($p < 0.001$). As described at 5 dpf, there was a significant effect of genotype on IOD ($F(2, 57) = 36.06, p < 0.001$) and ESD ($F(2, 57) = 4.454, p = 0.016$). Pairwise post-hoc analysis showed those changes to be driven by HET. While ESD was increased in the HET when compared to WT ($p = 0.026$), the IOD was diminished in the HET ($p < 0.001$) compared to WT. No other significant differences were observed.

Data related to *baz1b*^{ins35} LoF show differences with respect to the *baz1b*^{del44} LoF (shorter eye to snout distance in the *baz1b*^{ins35} mutants instead, Figure S3), suggesting that the two lines could be useful for different types of study.

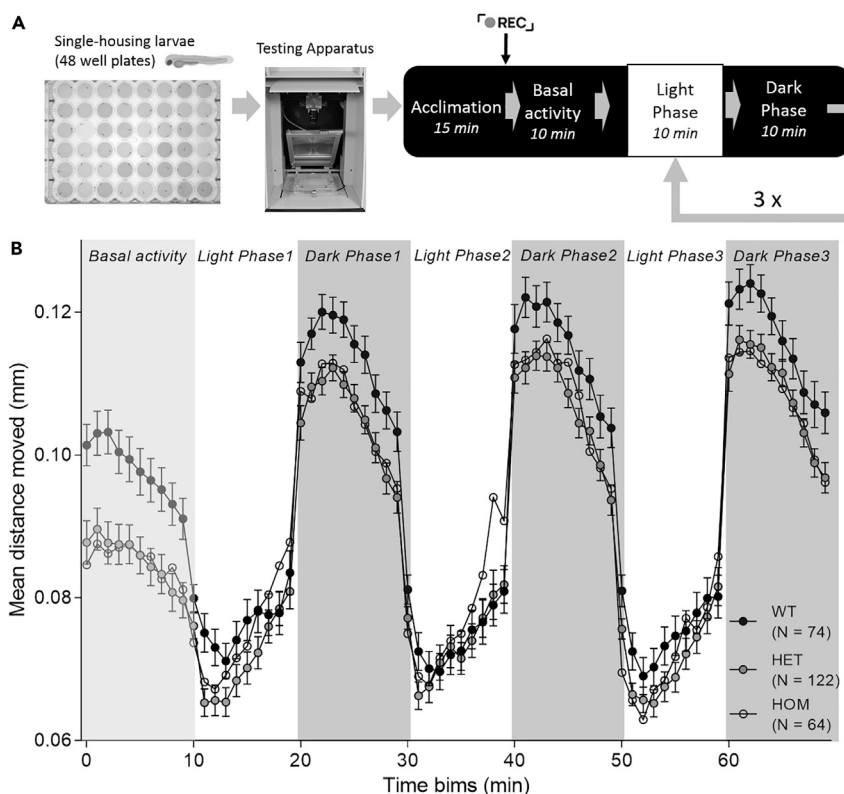


Figure 3. Loss of *baz1b* leads to faster habituation in the forced light-dark transition (FLDT) assay

(A) Diagram of the assay.

(B) Mean distance moved per genotype during the baseline and the three light-dark cycles (10 min each). Note that both HET and HOM describe a steeper slope than WT sibling during the light phases. Data show mean \pm SEM.

Loss of *baz1b* diminishes stress response and habituation in larval zebrafish

As *baz1b* LoF affected maturation of the neural crest and facial morphology consistent with the NCDS hypothesis, we next examined whether *baz1b* LoF also showed behavioral differences associated with DS. Larvae from the three possible genotypes were assessed for stress reactivity at 5 dpf using a forced light-dark transition (FLDT) assay and response to brief flash of light or acoustic startle.³¹

In both the FLDT and the flash of light paradigm, in the absence of differences in basal locomotion, distance traveled in the first 5 min following the exposure to bright light is used as a measure of anxiety-like response.^{32,33} In the FLDT, others have also used the rate of recovery between light transitions as a measure of anxiety-like response.³³ Here, during the initial basal stage of the FLDT assay, before the alternating light/dark cycles, there was a significant effect of genotype on locomotion ($F(2) = 8.62$, $p = 0.013$), where HET traveled shorter distances than the WT ($p = 0.013$). Although HOM showed a similar reduction in overall distance traveled, they did not reach significance when compared to WT ($p = 0.079$). This difference in distance traveled was maintained across all dark phases of the experiment such that there was a significant difference in distance traveled between HET and WT in dark ($p = 0.022$) and in total distances traveled ($p = 0.017$). Analysis of the rate of recovery following a change in light conditions revealed that *baz1b* LoF zebrafish recover more quickly than WT siblings suggesting a diminished stress response (Figure 3). The rate of increase in locomotion during the light periods, assessed as the combined slopes from the three light periods (first: minute 10 to 20, second: minute 30 to 40, third: minute 50 to 60), revealed a significant effect of time-genotype interaction (slope) ($F(2) = 229.84$, $p < 0.001$). Difference was observed between the mutant and WT, with the slope of HET and HOM being significantly steeper across the three light periods (HET: $p = 0.033$; HOM: $p = 0.028$). Dark periods, measured as a sum of slopes in dark periods that followed the light periods (first: minute 20 to 30, second: minute 40 to 50, third: minute 60 to 70) also revealed significant effect of time-genotype interaction ($F(2) = 7.94$, $p = 0.019$) such that HET recovered significantly faster than WT ($p = 0.024$). There was no difference between HOM and WT ($p = 0.189$).

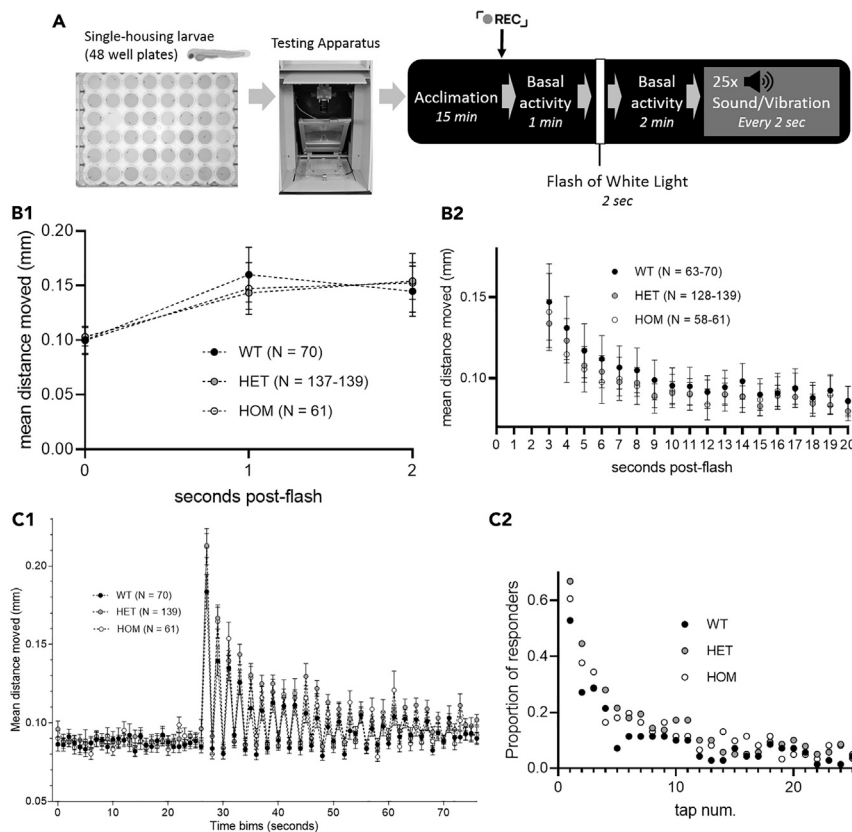


Figure 4. Loss of *baz1b* diminishes stress response and habituation in the flash of light and acoustic startle assay

(A) Diagram of the assay.

(B) Flash of light: total distance moved during the flash of light (time 0) and 2 s after. Dots represent distance traveled in 1 s time bins (B1), and mean distance moved during recovery for the 18 s following this period (B2). Dots represent 1 s time bins.

(C) Acoustic startle assay: total distance moved 25 s before and during the acoustic cues (C1) and proportion of responders during the acoustic cues (C2). In all cases, data show mean \pm SEM. Intragroup variations in N number are due to statistical exclusion criteria applied at each time bin.

Similar to the FLDT assay, analysis of the flash of light paradigm showed significant differences between *baz1b* LoF and WT fish (Figure 4B). The analysis of the baseline before the flash of light did not reveal significant differences between genotypes ($p > 0.05$). On transition from light to dark, in this assay, fish movement rapidly increases but the genotype was not an indicator of the height of the jump ($p > 0.05$). However, there was a significant effect of time-genotype interaction on the slope of recovery following the flash of light ($F(2) = 7.509$, $p = 0.023$) between the HOM and WT ($p = 0.009$) such that HOM recovered faster suggestive of a reduced stress response. No other comparisons were significant. We next assessed locomotion after recovery from the flash of light and before the acoustic stimuli started. As in the first basal period, there was no significant difference between the genotypes in locomotion ($p > 0.05$).

Next, we evaluated two parameters, distance traveled and proportion of responders, to assess the rate of habituation to a repeated acoustic startle. Defective startle habituation is associated with stress disorders.³¹ There were no significant differences in locomotion before the first tap stimulus, in magnitude of the response to the first tap stimulus, nor in total distance moved across all tap stimuli across experimental groups indicating that differences in startle behavior were not confounded by differences in locomotion *per se*. The total distance moved by fish during each TAP event was used to define the slope of habituation and a significant effect of genotype-tap number interaction was found ($F(2) = 8.42$, $p = 0.015$) (Figure 4C1). Mutant fish habituated more quickly than WT, again consistent with a reduction in stress reactivity, but the difference was significant only for HET fish (HET: $p = 0.011$; HOM: $p = 0.088$). We also assessed the habituation response to repeated acoustic startle stimulation by looking at the decrease in the proportion

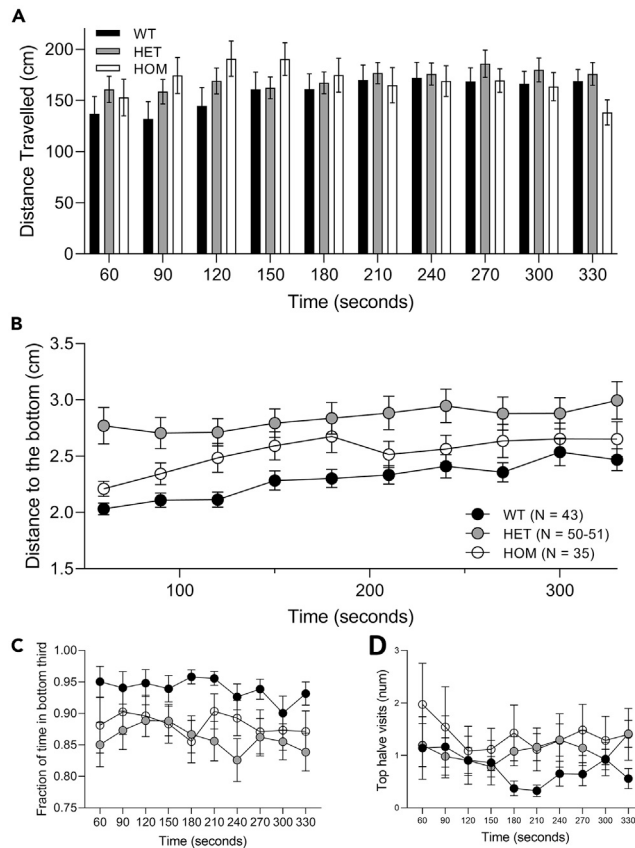


Figure 5. Novel tank diving assay shows anxiolytic phenotype in *baz1b* LoF zebrafish

(A) Changes in distance traveled for the three genotypes in the novel tank diving assay divided in 30 s time beams. (B) Distance to the bottom of the assay in each 30 s for the three genotypes. (C) Fraction of time in the bottom third and D) top half visits for the three genotypes during the novel tank diving assay. Graphs show mean \pm SEM. Intragroup variations in N number are due to statistical exclusion criteria applied at each time bin.

of responders across stimuli (Figure 4C2). Statistical analysis showed a significant effect of genotype ($F(2) = 29.283$, $p < 0.001$). Post-hoc analysis revealed that in both HET and HOM the decrease in the proportion of responders was significantly steeper than WT siblings (HET: $p < 0.001$; HOM: $p < 0.001$).

The second line generated, *baz1b*^{ins35}, shows similar results in the three behavioral assays (Figure S4).

Reduced anxiety-like behavior in *baz1b* LoF persists at later life stages

As both WS individuals and domesticated species show reduced stress reactivity throughout life, we also investigated if the diminished stress reactivity observed during early development in the *baz1b* LoF larvae was maintained at later stages. We used the novel tank diving assay, one of the most used behavioral tests to assess anxiety phenotypes in zebrafish, where time spent in the bottom third of the tank and distance from the bottom of the tank are used as measures of anxiety-like behavior,³⁴ to assess anxiety-driven responses of juvenile fish (10–12 weeks old; Figure 5).

There was a significant main effect of time ($F(9) = 9.085$, $p < 0.001$) and genotype ($F(2) = 7.336$, $p < 0.001$) on the distance to the bottom, but the interaction time-genotype failed to reach significance ($F(18) = 1.029$, $p = 0.421$). Distance from the bottom increased with time suggesting reduction in anxiety-like response throughout the time in the novel environment, which agrees with the normal response of fish to novelty. Genotype differences on the distance from the bottom were driven by HET fish spending significantly less time closer to the bottom than the other two genotypes (HET vs HOM: $p = 0.0126$; HET vs

WT: $p < 0.0001$; HOM vs WT: $p = 0.548$). Regarding total distance traveled, there were no significant effects of either genotype ($F(2) = 1.579$, $p = 0.212$) or time ($F(9) = 2.205$, $p = 0.190$).

When assessing the proportion of time spent on the bottom third of the tank (Figure 5C), we found no effect of time ($F(9) = 1.133$, $p = 0.361$), and no significant interaction between genotype and time ($F(18) = 0.246$, $p = 0.999$). However, there was a significant effect of genotype ($F(2) = 11.043$, $p < 0.001$). Post-hoc analysis revealed this to be driven by HET spending less time in the bottom third of the tank than WT (HET vs HOM: $p = 0.0704$; HET vs WT: $p < 0.0001$; HOM vs WT: $p = 0.079$). In contrast, we did not find a significant effect of genotype on the visits to the top half of the tank (Figure 5D; $F(2) = 2.415$, $p = 0.120$), while there was a significant effect of time ($F(9) = 3.118$, $p = 0.003$) and the interaction between genotype and time ($F(18) = 2.7$, $p < 0.001$) whereby mutant fish are quicker to make more top half visits than wild types after an initial reduction observed in all three genotypes.

Again, both HET and HOM *baz1b^{ins35}* mutants showed similar differences in behavior although this did not reach significance (Figure S5).

Loss of *baz1b* disturbs the ontogeny of social behavior in zebrafish

As the neural crest domestication hypothesis predicts an extension of the socialization window during development,^{16,17,35–37} we assessed the ontogeny of social behavior in *baz1b* LoF mutants (Figures 6 and S6). We used a method developed by Dreosti et al.³⁸ in which the preference to stay close to conspecifics is used as a measure of sociability. Assessing this behavior between 1 and 3 weeks of age, from non-social to fully developed social behavior respectively, allows comparison of the ontogeny of social behavior between genotypes.

Statistical analysis of the correlation indexes showed that there was a significant genotype-age of testing interaction on the social preference in the 0 vs. 3 contrast ($F(4, 554) = 4.130$, $p = 0.003$). In contrast, the interaction did not reach significance in the 0 vs. 1 contrast ($F(4, 556) = 0.06217$, $p = 0.993$).

None of the genotypes showed any significant preference for the social cues when presented with either contrast (0 vs. 3, or 0 vs. 1) during the first week of age and, consequently, no differences in the correlation indexes were detected (Figure S6A).

At 2 weeks of age (Figure 6), fish from all genotypes showed a significant tendency to remain in proximity to multiple conspecifics (0 vs. 3; WT: $W = -544.0$, $p = 0.0451$; HET: $W = -1618$, $p < 0.001$; HOM: $W = -770.0$, $p = 0.003$). Similarly, all genotypes showed this social preference when confronted with one conspecific (0 vs. 1; WT: $W = -733.0$, $p = 0.001$; HET: -911.0 , $p < 0.001$; HOM: -699.0 , $p = 0.002$). Statistical analysis of the correlation index revealed that there was a significant difference between genotypes ($H(6) = 17.22$, $p = 0.004$) and multiple comparisons revealed it to be driven by HET showing a greater motivation to interact with conspecifics than WT ($p = 0.005$) and HOM ($p = 0.011$) in the 0 vs. 3 contrast, while no differences were detected in the 0 vs. 1 contrast. There were no significant differences in the number of fish showing antisocial behavior (avoiding arm with conspecific/s).

At 3 weeks of age (Figure S6B), all genotypes showed a strong preference to interact with either multiple (0 vs. 3; WT: $W = -1966$, $p < 0.001$; HET: $W = -1596$, $p < 0.001$; HOM: $W = -1924$, $p < 0.001$) or single (0 vs. 1; WT: $W = -2286$, $p < 0.001$; HET: $W = -2563$, $p < 0.001$; HOM: $W = -2245$, $p < 0.001$) conspecifics and the statistical analysis of the correlation indexes did not describe any significant differences between genotypes ($H(6) = 452$, $p = 0.108$).

Thus, results of the sociability assay suggest that *baz1b* dosage influences the ontogeny of pro-social behaviors. Mutants of the *baz1b^{ins35}* line also showed altered social ontogeny, although with variations: HOM showed increased motivation to shoal at week 1 but decrease at 3 weeks of age (Figure S7).

DISCUSSION

Baz1b has been suggested to play a key role in the domestication process; however, although knockdown of *baz1b* is associated with effects on neural crest development and craniofacial changes consistent with a role in this process, a link between *baz1b* and behavioral changes associated with domestication has not been established. Thus, here we tested the hypothesis that *baz1b* regulates neural crest development and

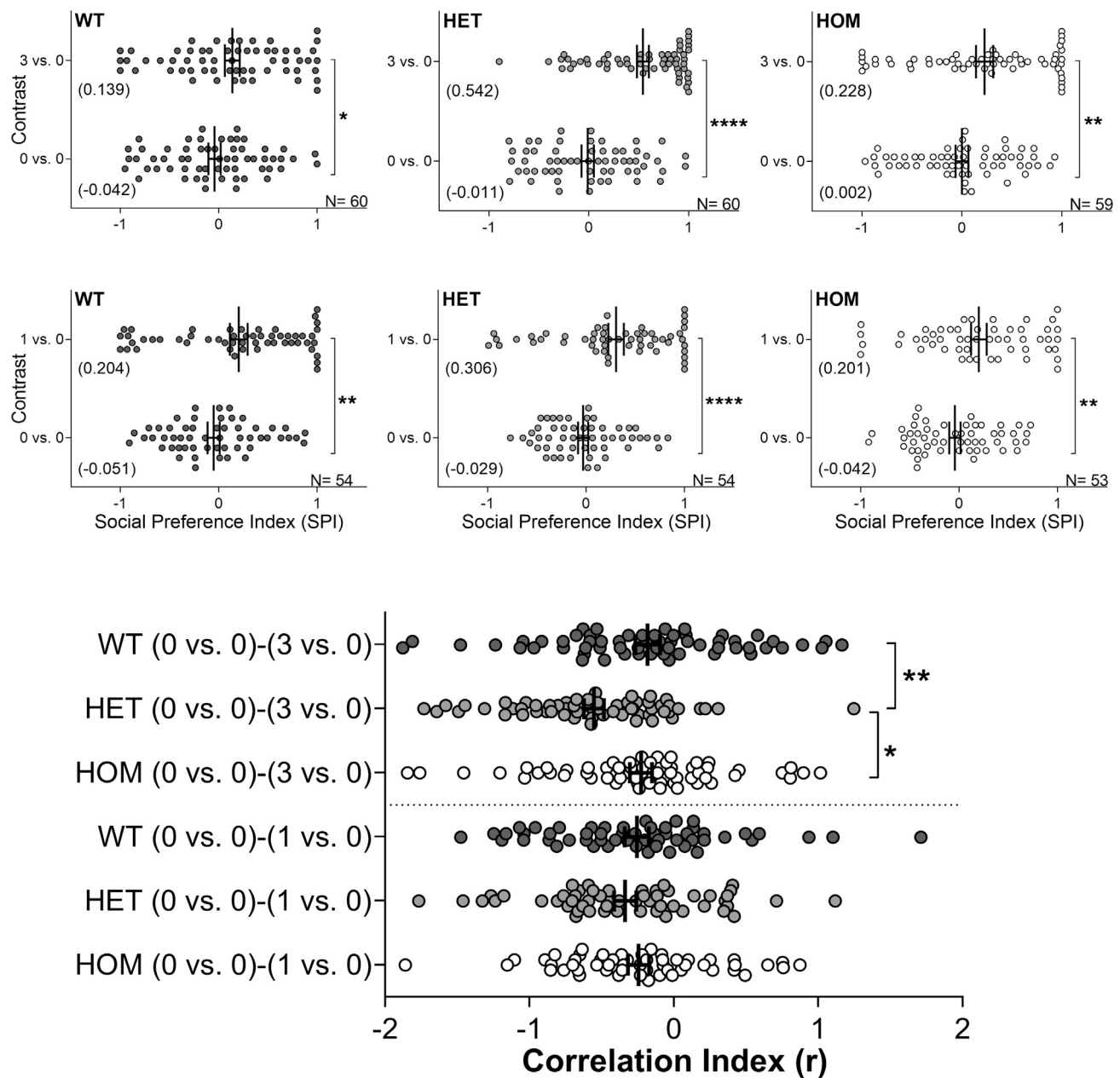


Figure 6. Loss of *baz1b* disturbs the ontogeny of sociability in zebrafish

Graphs show change in social preference index (SPI) between basal conditions (0 vs. 0) and contrast (0 vs. 3 or 0 vs. 1) for either WT, HET, or HOM at week 2 of age (for week 1 and 3 see Figure S6). N is included in each graph. Below panel shows the comparison of the correlation indexes for all the contrast at week 2 (from 13 to 15 dpf). Graphs show individual values and mean (also between brackets for SPI) \pm SEM. In all cases: * $p < 0.05$; ** $p < 0.01$; **** $p < 0.001$. Statistical test: non-parametric two-tailed Wilcoxon signed-rank test of paired samples for SPIs; non-parametric test of Kruskal-Wallis of not paired samples with Dunn's correction for multiple comparisons for correlation index.

both morphological and pro-social behavioral phenotypes associated with domestication using zebrafish as a model species. In agreement with previous data from *in vitro* human cells and other *in vivo* models, *baz1b* LoF resulted in mild developmental delay at earlier stages, disruption of neural crest development, and sustained craniofacial morphological differences later in life. Lack of *baz1b* also resulted in fish showing a diminished stress response and increased willingness to socialize with conspecifics during the ontogeny of social behavior.

Lack of functional *baz1b* resulted in minor morphological differences associated with mild developmental delay during early embryogenesis. Although in zebrafish mild developmental delay, as determined by the head-to-tail distance, resolved at around 24 hpf, both changes in pigmentation and reduced rate of hatching were observed at later stages, which is consistent with altered input of the neural crest to destination tissues: differential distribution of pigment cell within dermis and epidermis³⁹ and immature neuromuscular junction,⁴⁰ respectively.

In agreement with previous studies, expression of markers of neural crest development was disrupted in *baz1b* LoF compared to WT siblings. Both qPCR and ISH revealed an increased level of expression of *crestin*, a marker of pre-migratory neural crest, in *baz1b* mutants. In contrast, no changes in *foxd3* were observed indicating that, although *baz1b* LoF alters the maturation of the neural crest, it does not seem to affect neural crest formation and maintenance.⁴¹ Interestingly, the reduction in *sox2* expression seen on *BAZ1B* knockdown in neural crest cells and *Xenopus* embryos was seen in *baz1b* heterozygous fish but not in homozygous fish consistent with the heterozygous state more closely resembling the knockdown condition. Several morphological and behavioral phenotypes were also found to be more severely affected in heterozygous than homozygous mutants. As is often the case, it may be that in the complete absence of functional Baz1b, other factors are able to substitute for Baz1b protein function in the regulation of *sox2* expression and/or other aspects of development. Nonetheless, our gene expression analysis are consistent with a shift in the balance between pre-migratory and migratory neural crest cells toward an extended immaturity period of the neural crest in *baz1b* LoF embryos similar to that observed on knockdown of *baz1b* in *Xenopus* and neural crest stem cells.^{6,12}

Altered development of the neural crest is associated with altered craniofacial morphology. Consistent with a role of Baz1b in neural crest development, deficiencies in *baz1b* induced mild differences in cranial bones and facial features at both 5 and 30 dpf but did not affect the external maturity of the fish. In the main line of this study, *baz1b*^{del44}, the LoF led to a significant elongation between Meckel's cartilage and the ceratohyal bone and, consequently, an increase in the eye-snout distance in the heterozygous larvae. In contrast, differences in craniofacial features reported in the second line, *baz1b*^{ins35}, were associated with shortened snouts. Craniofacial features of flattened nasal bone, protruding forehead, and shorter snout are seen in *Baz1b* LoF mice and are similar to craniofacial features seen in patients with WS as well as some domesticated species.^{1,13} The difference in phenotypes seen in the two *baz1b* LoF lines suggests that, although *baz1b* dosage plays a role in the determination of facial features, other genes might be influencing the overall phenotype. This might explain why the reduction in facial features is sporadically reported in different species of domesticated animals despite variation at the *baz1b* locus.^{42–44}

A key aspect of our study was to test the hypothesis that reduction in expression of *baz1b* affected behaviors associated with domestication. We examined stress reactivity and social behavior. At both larval and juvenile stages, *baz1b* LoF led to a reduction of stress reactivity. At larval stages, mutant zebrafish showed increased rate of recovery in both the FLDT and light startle assay with no consistent effects on locomotion *per se*. In both FLDT and light flash startle paradigm, distance moved in the first 5 min following light to dark transition is used as an indicator of anxiety-like response such that the greater the distance traveled, the greater the anxiety.^{32,33} As in the FLDT baseline locomotion varied with genotype, distance traveled on light to dark transition is not informative. However, the rate of recovery following light to dark, and dark to light transition has also been used as a measure of anxiety-like response.³³ Using this measure, there is a difference in the rate of recovery such that mutants recover more quickly on all transitions. This finding is consistent with reduced anxiety rather than reduced locomotion, as if just reduced locomotion, a slower recovery in the light, and faster in the dark, would have been expected. The quick flash of light startle assay is an adaptation of that recently developed by Lee and colleagues³² which is shown to rely on hypothalamus-pituitary-interrenal (HPI) reactivity, the teleost equivalent of the mammalian HPA axis. Therefore, our data are consistent with reduced HPI response. The neural crest contributes to formation of the adrenal glands in both mammals and fish such that delay in maturation of the neural crest leads to reduced HPA/I response.^{17,44} Thus, the reduction in stress reactivity in *baz1b* mutants at larval stages is consistent with delayed maturation of HPI as predicted by our gene expression analysis and the NCDS hypothesis. Consistent with findings in domesticated species, these differences in stress reactivity persisted at later developmental stages; 30 dpf heterozygous and homozygous fish showed a reduction in the tank diving response, although this only reached significance for heterozygous fish.

As increased pro-social behavior is associated with *BAZ1B* deficiency in WS and with domestication, and the NCDS hypothesis predicts delayed maturation of the neural crest leads to prolonged socialization

window,^{14,43,44} we assessed the ontogeny of social behavior in larval and juvenile zebrafish. Our data showed that *baz1b* LoF resulted in an increased inclination to interact with conspecifics at 2 weeks of age. Furthermore, the sociability assay also shows that multiple, instead of single, conspecifics are stronger drivers of social behaviors in *baz1b* LoF zebrafish, which agrees with the NCDS hypothesis as this alteration will be favoring larger social groups and intraspecific interactions.^{18,45} Although *baz1b* LoF might not be influencing the overall time it takes to develop zebrafish' social skills, it seems to affect the eagerness to establish social contact with conspecifics during its ontogeny.

Differences in sociability are no longer observed by 3 weeks of age. However, the lack of differences could be a consequence of either a) all fish, regardless of genotype, have developed a similar level of sociability at this age thus suggesting differences observed at early stages have resolved or b) if differences in sociability remain, they cannot be detected in this assay as the salience to socialize is too strong by 3 weeks of age in all genotypes. Nonetheless, *Baz1b* might still be playing a role in social responses later in life as it has been implicated in stimulus-specific response to different emotional paradigms in rodents.⁴⁶

Taken all together, our research shows that in zebrafish *baz1b* regulates both morphological and behavioral phenotypes associated with the domestication syndrome in other species. This investigation therefore supports the NCDS hypothesis. Although extrapolations from zebrafish to other vertebrates and the process of domestication might be challenging, this animal model has repeatedly proven its validity in behavioral neuroscience.^{47,48}

Our work also suggests *BAZ1B* LoF plays a causal role in the increased sociability and craniofacial dimorphisms observed in individuals with WS. However, despite the social predisposition, increased anxiety and anxiety-related disorders are prevalent in WS,⁴⁹ which is at odds with the reduced anxiety response seen in *baz1b* LoF fish. Thus, our research suggests that *BAZ1B* is not a main contributor for this neurological feature in WS. Although the lack of functional *BAZ1B* might result in a mild underdevelopment of the HPA axis, other genes altered in this syndrome might have a more prominent role defining the final state of stress- and anxiety reactivity in WS. Therefore, this research emphasizes the need to assess the consequences of lacking specific genes alone to establish genotype-phenotype correlation when studying disorders spanning multiple genes such as WS.

As *Baz1b* acts as both a transcription factor and chromatin remodeler in the neural crest, it offers a powerful opportunity to extend the comparative studies to the epigenome. Targeting *Baz1b*-associated chromatin interactions by novel multi-omics approaches might help to elucidate the associated changes in gene expression. Thus, future studies that investigate how *Baz1b* regulates the epigenomic landscape can help to elucidate the set of regulatory changes leading toward pro-social behavior and the initial domestication-associated phenotypes.

Limitations of the study

Both lines used in this study revealed similar findings; however, there are some subtle differences. For example, *baz1b^{del44}* HETs showed both morphological and behavioral changes with HOMs being largely unchanged, whereas in *baz1b^{ins35}* both HETs and HOMs showed phenotypic changes but these were less marked than in *baz1b^{44del}*. This incongruence could be manifesting different penetrance of the mutation since the fold change of *baz1b* expression is minor in the second line with the reduced phenotype in *baz1b^{del44}* homozygous mutants reflecting partial rescue by substituting pathways. *BAZ1B* haploinsufficiency, as seen in WS, is associated with hyper-sociability^{7,50} while its duplication is linked to opposing behaviors such as autism-like features.^{4,5} Further, in contrast to zebrafish, total absence of *Baz1b* expression in rodents leads to mortality shortly after birth due to heart defects.^{12,51} Therefore, heterozygous individuals might reflect better both the human WS pathology and the genetic variations observed in domesticated species.

STAR★METHODS

Detailed methods are provided in the online version of this paper and include the following:

- KEY RESOURCES TABLE
- RESOURCE AVAILABILITY
 - Lead contact
 - Materials availability
 - Data and code availability

- EXPERIMENTAL MODEL AND SUBJECT DETAILS
- METHOD DETAILS
 - Generating loss-of-function (LoF) zebrafish
 - Quantitative PCR (qPCR)
 - Whole body *in situ* hybridization (WISH)
 - Alcian blue staining
 - Additional morpho-physiological measurements
 - Behavioural evaluation
- QUANTIFICATION AND STATISTICAL ANALYSIS
 - Molecular and morphological comparisons
 - Larval behavioural assays and novel tank diving
 - Ontogeny of sociability behaviour

SUPPLEMENTAL INFORMATION

Supplemental information can be found online at <https://doi.org/10.1016/j.isci.2022.105704>.

ACKNOWLEDGMENTS

We thank Dr Katharine E. Lewis for providing the *pax2b* probe. Funders: Human Frontiers Scientific Program (RGP 0008/2017, J.V.T.P., C.H.B.); National Institutes of Health (NIH U01 DA044400-03, A.M.M., W.H., C.H.B.); Leverhulme Trust (RPG-2016-143, S.A., CHB); European Commission (SPANUMBRA – 833504, S.A., C.H.B.); Ministerio de Universidades (Next Generation EU), Universitat de València, Ayudas Marra Zambrano para atraer talento internacional (ZA21-026, J.V.T.P.).

AUTHOR CONTRIBUTIONS

J.V.T.P.: conceived and planned experiments, lines generation, molecular and behavioral experiments, data analysis, writing and graphical abstract. S.A.: qPCR for markers for neural crest, morphological measurements and analysis. A.M.M.: analysis of 5 dpf behavioral data. W.H.: analysis of the novel tank data and part of the 5 dpf behavioral data. J.G.G.: assistance in line generation. S.E.F. and G.V.: provided funding. C.H.B.: provided funding, supervised the project and writing. All authors discussed the results and contributed to the final manuscript.

DECLARATION OF INTERESTS

Authors declare no conflict of interest.

INCLUSION AND DIVERSITY

We support inclusive, diverse, and equitable conduct of research.

Received: September 7, 2022

Revised: November 15, 2022

Accepted: November 29, 2022

Published: January 20, 2023

REFERENCES

1. Sharif, S.B., Zamani, N., and Chadwick, B.P. (2021). Baz1b the protean protein. *Genes* 12, 1541.
2. Martens, M.A., Wilson, S.J., and Reutens, D.C. (2008). Research Review: Williams syndrome: a critical review of the cognitive, behavioral, and neuroanatomical phenotype. *J. Child Psychol. Psychiatry* 49, 576–608.
3. Royston, R., Oliver, C., Howlin, P., and Waite, J. (2021). Anxiety characteristics in individuals with Williams syndrome. *J. Appl. Res. Intellect. Disabil.* 34, 1098–1107.
4. Mervis, C.B., Klein-Tasman, B.P., Huffman, M.J., Velleman, S.L., Pitts, C.H., Henderson, D.R., Woodruff-Borden, J., Morris, C.A., and Osborne, L.R. (2015). Children with 7q11.23 duplication syndrome: psychological characteristics. *Am. J. Med. Genet.* 167, 1436–1450.
5. López-Tobón, A., Trattaro, S., and Testa, G. (2020). The sociability spectrum: evidence from reciprocal genetic copy number variations. *Mol. Autism.* 11, 1–13.
6. Zanella, M., Vitriolo, A., Andirko, A., Martins, P.T., Sturm, S., O'Rourke, T., Laugsch, M., Malerba, N., Skaros, A., Trattaro, S., et al. (2019). Dosage analysis of the 7q11.23 Williams region identifies BAZ1B as a major human gene patterning the modern human face and underlying self-domestication. *Sci. Adv.* 5, eaaw7908.
7. Niego, A., and Benítez-Burraco, A. (2019). Williams syndrome, human self-domestication, and language evolution. *Front. Psychol.* 10, 521.
8. VonHoldt, B.M., Ji, S.S., Aardema, M.L., Stahler, D.R., Udell, M.A.R., and Sinsheimer, J.S. (2018). Activity of genes with functions in human Williams-Beuren syndrome is impacted by mobile element insertions in the

- gray wolf genome. *Genome Biol. Evol.* 10, 1546–1553.
9. Lu, X., Meng, X., Morris, C.A., and Keating, M.T. (1998). A novel human gene, WSTF, is deleted in Williams syndrome. *Genomics* 54, 241–249.
 10. Cus, R., Maurus, D., and Köhl, M. (2006). Cloning and developmental expression of WSTF during *Xenopus laevis* embryogenesis. *Gene Expr. Patterns* 6, 340–346.
 11. Lalli, M.A., Jang, J., Park, J.H.C., Wang, Y., Guzman, E., Zhou, H., Audouard, M., Bridges, D., Tovar, K.R., Papuc, S.M., et al. (2016). Haploinsufficiency of BAZ1B contributes to Williams syndrome through transcriptional dysregulation of neurodevelopmental pathways. *Hum. Mol. Genet.* 25, 1294–1306.
 12. Barnett, C., Yazgan, O., Kuo, H.C., Malakar, S., Thomas, T., Fitzgerald, A., Harbour, W., Henry, J.J., and Krebs, J.E. (2012). Williams Syndrome Transcription Factor is critical for neural crest cell function in *Xenopus laevis*. *Mech. Dev.* 129, 324–338.
 13. Ashe, A., Morgan, D.K., Whitelaw, N.C., Bruxner, T.J., Vickaryous, N.K., Cox, L.L., Butterfield, N.C., Wicking, C., Blewitt, M.E., Wilkins, S.J., et al. (2008). A genome-wide screen for modifiers of transgene variegation identifies genes with critical roles in development. *Genome Biol.* 9, R182.
 14. Wilkins, A.S., Wrangham, R.W., and Fitch, W.T. (2014). The “domestication syndrome” in mammals: a unified explanation based on neural crest cell behavior and genetics. *Genetics* 197, 795–808.
 15. Thomas, J., and Kirby, S. (2018). Self domestication and the evolution of language. *Biol. Philos.* 33, 9.
 16. Wright, D. (2015). The genetic architecture of domestication in animals. *Bioinform. Biol. Insights* 9, 11–20.
 17. Sánchez-Villagra, M.R., Geiger, M., and Schneider, R.A. (2016). The taming of the neural crest: a developmental perspective on the origins of morphological covariation in domesticated mammals. *R. Soc. Open Sci.* 3, 160107.
 18. Šimić, G., Vukić, V., Kopic, J., Krsnik, Ž., and Hof, P.R. (2020). Molecules, mechanisms, and disorders of self-domestication: keys for understanding emotional and social communication from an evolutionary perspective. *Biomolecules* 11, 2.
 19. Parker, M.O., Brock, A.J., Walton, R.T., and Brennan, C.H. (2013). The role of zebrafish (*Danio rerio*) in dissecting the genetics and neural circuits of executive function. *Front. Neural Circuits* 7, 63.
 20. Bradford, Y.M., Toro, S., Ramachandran, S., Ruzicka, L., Howe, D.G., Eagle, A., Kalita, P., Martin, R., Taylor Moxon, S.A., Schaper, K., et al. (2017). Zebrafish models of human disease: gaining insight into human disease at ZFIN. *ILAR J.* 58, 4–16.
 21. Nicholson, P., and Mühlemann, O. (2010). Cutting the nonsense: the degradation of PTC-containing mRNAs. *Biochem. Soc. Trans.* 38, 1615–1620.
 22. Klymkowsky, M.W., Rossi, C.C., and Artinger, K.B. (2010). Mechanisms driving neural crest induction and migration in the zebrafish and *Xenopus laevis*. *Cell Adh. Migr.* 4, 595–608.
 23. Kelly, G.M., and Moon, R.T. (1995). Involvement of Wnt1 and Pax2 in the formation of the midbrain-hindbrain boundary in the zebrafish gastrula. *Dev. Genet.* 17, 129–140.
 24. Zhang, S., and Cui, W. (2014). Sox2, a key factor in the regulation of pluripotency and neural differentiation. *World J. Stem Cells* 6, 305–311.
 25. McLennan, R., and Krull, C.E. (2002). Ephrin-As cooperate with EphA4 to promote trunk neural crest migration. *Gene Expr.* 10, 295–305.
 26. Wakamatsu, Y., and Uchikawa, M. (2021). The many faces of Sox2 function in neural crest development. *Dev. Growth Differ.* 63, 93–99.
 27. Gebuijs, I.G.E., Raterman, S.T., Metz, J.R., Swanenberg, L., Zethof, J., Van Den Bos, R., Carels, C.E.L., Wagener, F.A.D.T.G., and Von Den Hoff, J.W. (2019). Fgf8a mutation affects craniofacial development and skeletal gene expression in zebrafish larvae. *Biol. Open* 8, bio039834.
 28. Staal, Y.C.M., Meijer, J., van der Kris, R.J.C., de Bruijn, A.C., Boersma, A.Y., Gremmer, E.R., Zwart, E.P., Beekhof, P.K., Slob, W., and van der Ven, L.T.M. (2018). Head skeleton malformations in zebrafish (*Danio rerio*) to assess adverse effects of mixtures of compounds. *Arch. Toxicol.* 92, 3549–3564.
 29. Leung, G.K.C., Luk, H.M., Tang, V.H.M., Gao, W.W., Mak, C.C.Y., Yu, M.H.C., Wong, W.L., Chu, Y.W.Y., Yang, W.L., Wong, W.H.S., et al. (2018). Integrating functional analysis in the next-generation sequencing diagnostic pipeline of RASopathies. *Sci. Rep.* 8, 2421.
 30. Singleman, C., and Holtzman, N.G. (2014). Growth and maturation in the zebrafish, *Danio rerio*: a staging tool for teaching and research. *Zebrafish* 11, 396–406.
 31. Beppi, C., Beringer, G., Straumann, D., and Bögli, S.Y. (2021). A model-based quantification of startle reflex habituation in larval zebrafish. *Sci. Rep.* 11, 22410.
 32. Lee, H.B., Schwab, T.L., Sigafoos, A.N., Gauker, J.L., Krug, R.G., Serres, M.R., Jacobs, D.C., Cotter, R.P., Das, B., Petersen, M.O., et al. (2019). Novel zebrafish behavioral assay to identify modifiers of the rapid, nongenomic stress response. *Gene Brain Behav.* 18, e12549.
 33. García-González, J., de Quadros, B., Havelange, W., Brock, A.J., and Brennan, C.H. (2021). Behavioral effects of developmental exposure to jwh-018 in wild-type and disrupted in schizophrenia 1 (Disc1) mutant zebrafish. *Biomolecules* 11, 319.
 34. Blaser, R.E., and Rosemberg, D.B. (2012). Measures of anxiety in zebrafish (*Danio rerio*): dissociation of black/white preference and novel tank test. *PLoS One* 7, e36931.
 35. Lazzaroni, M., Range, F., Backes, J., Portele, K., Scheck, K., and Marshall-Pescini, S. (2020). The effect of domestication and experience on the social interaction of dogs and wolves with a human companion. *Front. Psychol.* 11, 785.
 36. Hansen Wheat, C., Fitzpatrick, J.L., Rogell, B., and Temrin, H. (2019). Behavioural correlations of the domestication syndrome are decoupled in modern dog breeds. *Nat. Commun.* 10, 2422.
 37. Ghazanfar, A.A., Kelly, L.M., Takahashi, D.Y., Winters, S., Terrett, R., and Higham, J.P. (2020). Domestication phenotype linked to vocal behavior in marmoset monkeys. *Curr. Biol.* 30, 5026–5032.e3.
 38. Dreosti, E., Lopes, G., Kampff, A.R., and Wilson, S.W. (2015). Development of social behavior in young zebrafish. *Front. Neural Circuits* 9, 39.
 39. Lister, J.A. (2002). Development of pigment cells in the zebrafish embryo. *Microsc. Res. Tech.* 58, 435–441.
 40. Tintignac, L.A., Brenner, H.R., and Rüegg, M.A. (2015). Mechanisms regulating neuromuscular junction development and function and causes of muscle wasting. *Physiol. Rev.* 95, 809–852.
 41. Teng, L., Mundell, N.A., Frist, A.Y., Wang, Q., and Labosky, P.A. (2008). Requirement for Foxd3 in the maintenance of neural crest progenitors. *Development* 135, 1615–1624.
 42. Lord, K.A., Larson, G., Coppinger, R.P., and Karlsson, E.K. (2020). The history of farm foxes undermines the animal domestication syndrome. *Trends Ecol. Evol.* 35, 125–136.
 43. Johnsson, M., Henriksen, R., and Wright, D. (2021). The neural crest cell hypothesis: no unified explanation for domestication. *Genetics* 219, iyab097.
 44. Wilkins, A.S., Wrangham, R., and Fitch, W.T. (2021). The neural crest/domestication syndrome hypothesis, explained: reply to Johnsson, Henriksen, and Wright. *Genetics* 219, iyab098.
 45. Hare, B. (2017). Survival of the friendliest: *Homo sapiens* evolved via selection for prosociality. *Annu. Rev. Psychol.* 68, 155–186.
 46. Sun, H., Martin, J.A., Werner, C.T., Wang, Z.J., Damez-Werno, D.M., Scobie, K.N., Shao, N.Y., Dias, C., Rabkin, J., Koo, J.W., et al. (2016). BAZ1B in nucleus accumbens regulates reward-related behaviors in response to distinct emotional stimuli. *J. Neurosci.* 36, 3954–3961.
 47. Levin, E.D., and Cerutti, D.T. (2009). Behavioral Neuroscience of Zebrafish. In *Methods of Behavior Analysis in Neuroscience*, Second edition, J.J. Buccafusco, ed. (CRC Press/Taylor & Francis).
 48. Shams, S., Rihel, J., Ortiz, J.G., and Gerlai, R. (2018). The zebrafish as a promising tool for modeling human brain disorders: a review

based upon an IBNS Symposium. *Neurosci. Biobehav. Rev.* **85**, 176–190.

49. Ng-Cordell, E., Hanley, M., Kelly, A., and Riby, D.M. (2018). Anxiety in Williams syndrome: the role of social behaviour, executive functions and change over time. *J. Autism Dev. Disord.* **48**, 796–808.
50. Kozel, B.A., Barak, B., Kim, C.A., Mervis, C.B., Osborne, L.R., Porter, M., and Pober, B.R. (2021). Williams syndrome. *Nat. Rev. Dis. Primers* **7**, 42.
51. Osborne, L.R. (2010). Animal models of Williams syndrome. *Am. J. Med. Genet. C Semin. Med. Genet.* **154C**, 209–219.
52. Kossack, M.E., and Draper, B.W. (2019). Genetic regulation of sex determination and maintenance in zebrafish (*Danio rerio*). *Curr. Top. Dev. Biol.* **134**, 119–149.
53. Keatinge, M., Tsarouchas, T.M., Munir, T., Porter, N.J., Larraz, J., Gianni, D., Tsai, H.H., Becker, C.G., Lyons, D.A., and Becker, T. (2021). CRISPR gRNA phenotypic screening in zebrafish reveals pro-regenerative genes in spinal cord injury. *PLoS Genet.* **17**, e1009515.
54. Evans, J.R., Torres-Pérez, J.V., Miletto Petrazzini, M.E., Riley, R., and Brennan, C.H. (2021). Stress reactivity elicits a tissue-specific reduction in telomere length in aging zebrafish (*Danio rerio*). *Sci. Rep.* **11**, 339.
55. Thisse, C., and Thisse, B. (2008). High-resolution in situ hybridization to whole-mount zebrafish embryos. *Nat. Protoc.* **3**, 59–69.
56. Kimmel, C.B., Ballard, W.W., Kimmel, S.R., Ullmann, B., and Schilling, T.F. (1995). Stages of embryonic development of the zebrafish. *Dev. Dyn.* **203**, 253–310.
57. Durbin, L., Brennan, C., Shiomi, K., Cooke, J., Barrios, A., Shanmugalingam, S., Guthrie, B., Lindberg, R., and Holder, N. (1998). Eph signaling is required for segmentation and differentiation of the somites. *Genes Dev.* **12**, 3096–3109.
58. Juárez-Morales, J.L., Schulte, C.J., Pezoa, S.A., Vallejo, G.K., Hilinski, W.C., England, S.J., de Jager, S., and Lewis, K.E. (2016). Evx1 and Evx2 specify excitatory neurotransmitter fates and suppress inhibitory fates through a Pax2-independent mechanism. *Neural Dev.* **11**, 1–20.
59. Blanco, A.M., Bertucci, J.I., Hatef, A., and Unniappan, S. (2020). Feeding and food availability modulate brain-derived neurotrophic factor, an orexigen with metabolic roles in zebrafish. *Sci. Rep.* **10**, 10727.
60. Martínez, R., Navarro-Martin, L., Luccarelli, C., Codina, A.E., Raldúa, D., Barata, C., Tauler, R., and Piña, B. (2019). Unravelling the mechanisms of PFOS toxicity by combining morphological and transcriptomic analyses in zebrafish embryos. *Sci. Total Environ.* **674**, 462–471.
61. Elabd, S., Jabeen, N.A., Gerber, V., Peravali, R., Bourdon, J.C., Kancherla, S., Vallone, D., and Blattner, C. (2019). Delay in development and behavioural abnormalities in the absence of p53 in zebrafish. *PLoS One* **14**, e0220069.

STAR★METHODS

KEY RESOURCES TABLE

REAGENT or RESOURCE	SOURCE	IDENTIFIER
Chemicals, peptides, and recombinant proteins		
tracrRNA	Sigma	Cat#TRACRRNA05N
Cas9 protein	New England Biolabs	Cat#M0386M
1-Phenyl-2-thiourea (PTU)	Sigma	CAS: 103-85-5
Alcian Blue	Sigma	CAS: 33864-99-2
Critical commercial assays		
QIAquick Gel Extraction kit	Quiagen	Cat#28706X4
pGEM-T Easy vector	Promega	Cat# A1360
Deposited data		
Raw, analyzed data and code	This paper; Mendeley Data	https://doi.org/10.17632/ktxyzdvwyyw.1
Experimental models: Organisms/strains		
Zebrafish (<i>Danio rerio</i>): Strain: Tübingen (TU); Mutation: baz1b_e5[44bp del]	Queen Mary University of London	Ximbio: baz1b_e5[44bp del] Zebrafish
Zebrafish (<i>Danio rerio</i>): Strain: Tübingen (TU); Mutation: baz1b_e5[35bp ins]	Queen Mary University of London	Ximbio: baz1b_e5[35bp ins] Zebrafish
Oligonucleotides		
crRNA, 5'CUCAUCCUCCACCCAGG, ensembl gene ID: ENSDART00000158503.2	This paper	N/A
Primers used for genotyping: forward 5' AGAAGAAGAAATGGGTCATGCC	This paper	N/A
Primers used for genotyping: reverse 5' CCTCTAAACCATCTCACCTTGT	This paper	N/A
Primers for qPCR, see Table S1	This paper	N/A
Primers for WISH, see Table S2	This paper	N/A
Software and algorithms		
Leica Application Suite LAZ EZ version 3.4.0	Leica Microsystems	https://www.leica-microsystems.com/
ImageJ Java 1.8.0_45 [64-bit]	Rasband, W.S., ImageJ, U. S. National Institutes of Health, Bethesda, Maryland, USA	https://imagej.nih.gov/ij/ , 1997-2018
Leica Application Suite X version 3.4.2.18368	Leica Microsystems	https://www.leica-microsystems.com/
Ethovision XT software	Noldus Information Technology, Wageningen, NL	RRID:SCR_000441
R Project for Statistical Computing version 4.0.0	R Project for Statistical Computing	RRID:SCR_001905
Rstudio version 1.2.5042	250 NORTHERN AVE, BOSTON, MA 02210	RRID:SCR_000432
GraphPad Prism 9.0.2 for Windows	GraphPad Software, San Diego, California USA	RRID:SCR_002798

RESOURCE AVAILABILITY

Lead contact

Further information and requests for resources, zebrafish or other resources should be directed to and will be fulfilled by the lead contact, Caroline H. Brennan (c.h.brennan@qmul.ac.uk).

Materials availability

Zebrafish lines generated in this study have been deposited to Ximbio (London, UK): baz1b_e5[44bp del] Zebrafish; baz1b_e5[35bp ins] Zebrafish. Additionally, zebrafish lines can be provided upon email request to the [lead contact](#).

Data and code availability

- All original data, statistics and codes used in this manuscript are available at Mendeley Data. <https://doi.org/10.17632/ktxyzdvwyyw.1>.
- Any additional information required to reanalyze the data reported in this paper is available from the [lead contact](#) upon request.

EXPERIMENTAL MODEL AND SUBJECT DETAILS

All *in vivo* experimental procedures described were reviewed and approved by the QMUL ethics committee (AWERB) following consultation of the ARRIVE guidelines (NC3Rs, UK) and conducted in accordance with the Animals (Scientific Procedures) Act, 1986 and Home Office Licenses.

Zebrafish were housed in a recirculating system (Techniplast, UK) with a light:dark cycle of 14:10. Both housing tanks and testing rooms were maintained at ~25–28°C. Subjects were maintained in aquarium-treated water and fed twice daily with dry food (ZM-400, Zebrafish Management Ltd, Winchester, United Kingdom) in the morning and live brine shrimp (*Artemia salina*) in the afternoon. All zebrafish used from this study originated from a Tübingen wild type (WT) background line.

To breed them, zebrafish were moved to breeding tanks with perforated floors in the evening and eggs collected the following morning. Eggs were incubated in groups of no more than 50 per Petri dish at 28°C until 5 dpf. At 6 dpf, larvae were transferred to the recirculating system and fed twice daily with commercial fry food (ZM-75, ZM-100, Zebrafish Management Ltd, Winchester, United Kingdom) and life paramecium/brine shrimp, depending on their age.

Sex in laboratory zebrafish lines is not determined by a chromosomal mechanism and sexual differentiation only initiates at ~25 dpf.⁵² Therefore, sex was not reported in the present study.

METHOD DETAILS

Generating loss-of-function (LoF) zebrafish

The procedure used is similar to that described by Keatinge and colleagues⁵³ but with small variations. One-cell stage zebrafish embryos were injected into the yolk with 1 nL injection solution containing 62.5 ng/μL crRNA (crRNA, Sigma), 62.5 ng/μL tracrRNA (Sigma, cat. TRACRRNA05N), 1:8 dilution Cas9 protein (New England Biolabs, cat. M0386M; diluted in buffer B, New England Biolabs, cat. B802S) and 1:40 dilution of phenol red (Sigma Aldrich). The crRNA (5'CUCAUCCUCCACCACCCAGG) was designated to target a section of exon 5 of the zebrafish gene *baz1b* (ensembl gene ID: ENSDART00000158503.2) overlapping a restriction site for the Bsl1 enzyme (New England Bioscience) which includes a PAM site. Once a pair of founders was identified (outcrossing them to WT and genotyping the offspring by PCR) they were in-crossed and resulting F1 genotyped. All identified homozygous individuals (*baz1b*^{-/-}) from the F1 were individually outcrossed with different non-related WT fish, eggs collected and combined to randomly select a population of heterozygous (*baz1b*^{+/-}) zebrafish to constitute the F2 (minimum of two tanks of 50 individuals each). Finally, F2s were in-crossed and F3 genotyped to establish a breeding stock of fish from each genotype. Primers used for genotyping: forward 5' AGAAGAAGAAATGGGTCATGCC and reverse 5' CCTCTTAAACCATCTCACCTTGT.

Quantitative PCR (qPCR)

To validate the LoF lines, groups of 16 larvae at 5 dpf from all corresponding genotypes (N = 3 per genotype) were collected and stored in RNAlater (Thermo Fisher) until use. Collected larvae were previously scrutinized to ensure consistent developmental stages across groups. RNA extraction and quantitative PCR (qPCR) were carried similarly as previously described.⁵⁴ The relative expression of *baz1b* (targeting exon 1 and 2, upstream of the mutation site) was calculated with two housekeeping genes (*β-actin* and *rpl13a*) as references, adjusted by their corresponding efficiencies and normalised similarly as done before.⁵⁴

Additional qPCR experiments were done under similar condition except using 24 hpf embryos instead of 5 dpf. Two experimental batches, at relevant embryological stages, were used for this characterisation. First batch to assess *crestin*, *sox2* and *sox10*. Second batch for *foxd3* and *p75NTRb*.

Specific sequence and additional details (length, efficiency, and source) can be found in [Table S1](#).

Whole body *in situ* hybridization (WISH)

We used a standard method for *in situ* hybridizations.⁵⁵ All embryos of 26 hpf or older were raised in fish water containing 200 μ M 1-Phenyl-2-thiourea (PTU; Sigma Aldrich) to prevent melanin synthesis. A minimum of 15 individuals per genotype and RNA probe were carefully staged before WISH using Kimmel's criteria⁵⁶ to ensure potential differences were due to genotype and not developmental delay. RNA probes were generated and amplified by PCR from cDNA produced similarly as above from WT larval tissue. PCR products were isolated with a QIAquick Gel Extraction kit (Quiagen) and purified fragments cloned into pGEM-T Easy vector (Promega). Specific details for the generated probes can be found in [Table S2](#). cDNA clones for the following probes were obtained from others: *epha4*⁵⁷ and *pax2b*.⁵⁸ Pictures were taken using a Leica S9i stereo microscope with an integrated CMOS camera (10Mpixels, pixel size 1.67 μ m \times 1.67 μ m), in a laptop Dell Latitude E5440 with the software Leica Application Suite LAZ EZ version 3.4.0 and stored as tagged image file format (tiff).

Alcian blue staining

5 dpf larvae were fixed overnight in 4% paraformaldehyde (PFA) in a phosphate-buffered solution with 0.1% Tween-20 (PBT; Sigma-Aldrich). Following day, larvae were washed with PBT, depigmented with a PBT solution containing 30% H₂O₂/0.5% KOH for approximately 1 hour, washed further with PBT, stained in 0.37% HCl/70% ethanol/0.1% Alcian blue in PBT for 90 minutes and washed again with 1% HCl/70% ethanol in PBT. Larvae were then cleared with 50% glycerol/0.5% KOH and mounted in a groove cut into a 1% agarose base at the bottom of a Petri dish to ensure consistent orientation of all larvae. Pictures taken from the ventral and lateral planes and analysed using software ImageJ Java 1.8_0_45 [64-bit] (Rasband, W.S., ImageJ, U. S. National Institutes of Health, Bethesda, Maryland, USA, <https://imagej.nih.gov/ij/>, 1997-2018). Bone measurements were selected from those used in previous published works,²⁷⁻²⁹ aiming to assess craniofacial changes in zebrafish: 1) width of the ceratohyal (CH) at palatooquadrate (PQ) joint; 2) length of (1) to Meckel's cartilage (M); 3) length M-CH; 4) width M at PQ joint; 5) M-PQ angle; and 6) CH angle. Relevant ratios of these measurements were also used whenever appropriate to assess craniofacial defects.²⁹

Additional morpho-physiological measurements

To ensure any observed differences are due to *baz1b* LoF and not background genetic differences between pairs, multiple individual breeding pairs (minimum of 10 per desired genotype) were set to breed simultaneously to obtain fish from the three possible genotypes (WT \times WT, HOM \times HOM and WT \times HOM). 30 minutes after breeding, all eggs were collected, pooled together according to genotype and 150 fertilized eggs selected at random from each genotype for morphophysiological analysis. 50 4-8 cell fertilised eggs were collected into each of 3 Petri dishes for each genotype to avoid possible 'plate-induced' differences. Pictures were taken at different stages using a Leica TL3000 Ergo microscope with a Leica DFC3000 G camera, the software Leica Application Suite X version 3.4.2.18368 and collected as tiff. In accordance with previously published analyses,⁵⁹ the following morphological analysis were performed using ImageJ: head-to-tail distance at 12 and 15 hpf, whole body length (BL) and portion of tail protruding from yolk sack at 24 hpf, relative pigmentation intensity at 30 hpf, and BL at 60 and 72 hpf. Additionally, the percentage of hatched larvae was monitored between 49 to 73 hpf.

At 5 dpf, some larvae (N = 30 per genotype) were fixed overnight with PFA. Following morning, larvae were briefly washed with PBST and cleared with increasing concentrations of glycerol up to 100%. Whole body dorsal and lateral plane pictures were taken using the same setup as in the Alcian blue section to measure similar parameters as assessed in Martinez et al., 2019⁶⁰: BL, eye length (EL), eye-snout distance (ESD), eye width (EW), head-trunk angle (HTA), head width (HW) and inter-ocular distance (IOD). 30 dpf fish were processed likewise, but without clearing with glycerol, to measure BL, EL, ESD, EW, HTA, HW and IOD, and to assess their maturity state based on pigmentation/maturation patterns similarly as Singleman & Holtzman 2014.³⁰ The analysis of the partial body measurements were done after standardising by BL (specific measurement/BL) to ensure directionality (increase vs. decrease; elongation vs. shortening) of the potential changes in the craniofacial features.

To ensure observed differences were not due to angle variations of the samples when taking pictures, fixed fish were positioned on a grooved area carved out of a 1% agarose base at the bottom of the Petri dishes.

Behavioural evaluation

Larvae used for behavioural assays were obtained from in-crosses of *baz1b* heterozygous (HET x HET) zebrafish and thus examiner was blind to genotype until larvae were culled and genotyped by PCR (similar to above) after behavioural experimentation.

Forced light-dark transition (FLDT) at 5 dpf

This test was performed between 9 am and 4 pm. 5 dpf larvae were individually placed in 48-well plates and set to acclimate for 15 minutes inside the dark DanioVision Observation Chamber (Noldus Information Technology, Wageningen, The Netherlands). After this period, an initial 10-minute recording in the dark (infrared conditions) was used as baseline and zebrafish larvae were subjected to 3 consecutive forced light/dark transition cycles, each consisting of 10 minutes of light followed by 10 minutes of dark. Distance travelled was recorded using Ethovision XT software (Noldus Information Technology, Wageningen, NL) and data were outputted in 10-second time bins. To account for experimental variation, two independent experiments per day were conducted on three consecutive days.

Flash of light and acoustic startle habituation at 5 dpf

Sensorimotor startle response and habituation were tested in a protocol combining a variation of the light-locomotor behavioural assay developed by Lee and colleagues³² and a startle tap test. This assay was performed between 9 am and 4 pm. At the beginning of each trial, individual 5 dpf larvae resulting from *baz1b* heterozygous in-crosses (unknown genotypes until the end of the experiment) were randomly placed in a 48-well plate and set to acclimate inside a dark DanioVision Chamber. After 10 minutes of initial habituation, recording started. Following a further minute of acclimation in the dark, larval zebrafish were exposed to a brief illumination in white light (2 seconds), and then back to dark conditions for 2 minutes. Right after, zebrafish larvae were subjected to 25 sound/vibration consecutive stimuli with an inter-stimulus interval of 2 seconds. Distance travelled was recorded using Ethovision XT software and data were outputted in one-second time bins. Two independent experiments per day were conducted in three consecutive days.

Novel tank diving assay of juvenile zebrafish

This assay was performed as described previously⁵⁴ with small adaptation for juvenile fish. Zebrafish were housed in tanks according to genotype. At least two batches of fish were used per genotype (to avoid tank effect) at 10-12 weeks old. This assay was conducted between 9 am and 2 pm. All zebrafish were fed between 30 to 60 minutes before testing started. Trapezoid tank dimensions were 22 (bottom part) x 27 (top part) x 9 x 14.5 cm. It contained 2 litres of fresh fish system water (10 cm height water column) that was changed between trials. Fish were individually placed in the test tank and recorded from the side for 6 minutes. Swimming activity, including distance to the bottom and total motility (distance moved by the subject, in cm, for each time bin), were tracked and analysed using EthoVision software and data outputted in 30-seconds time bins.

Ontogeny of sociability

This assay was performed as Dreosti et al. 2015³⁸ with small modifications. Briefly, 4 tanks of 50 fish were kept for each genotype and re-analysed at weeks one (6 to 8 dpf), two (13 to 15 dpf) and three (20 to 22 dpf). Tests were performed between 10 am and 7 pm. Each fish was only tested once within each week, with a delay between consecutive weeks of testing of ≥ 7 days. Fish used as test subjects from each genotype were age/size matched to stimuli fish from the same genotype (same housing tank). Experiments were performed simultaneously in two DanioVision Observation Chambers, each containing 6 arena setups with fish from a certain genotype. At least two independent experiments were conducted each day per genotype and DanioVision Chamber with side of social cue presentation balanced in each trial. Swimming activity, including total motility and position within the arena, were tracked and analysed using EthoVision XT software and data outputted in single 15 minutes bins. Social Preference Index (SPI) was calculated similarly to Dreosti et al. 2015 but, additionally, we calculated the Correlation Index (r) to compare predisposition of fish to socialize: [$r = \text{SPI}_{\text{ExperimentalPhase}} - \text{SPI}_{\text{AcclimationPeriod}}$].

QUANTIFICATION AND STATISTICAL ANALYSIS

Power calculations (beta = 0.8, alpha = 0.05), with effect sizes determined from pilot studies, were used to estimate sample size for each experiment. The N number for each experiment can be found in the

corresponding figure or provided supplementary materials. Whenever possible, animals/contrast/testing order were selected at random. Unless stated otherwise, all effects are reported as significant at $p < 0.05$.

Molecular and morphological comparisons

The qPCR data on relative change in gene expression and all morphological comparisons were analysed using GraphPad Prism 9.0.2 for Windows (GraphPad Software, San Diego, California USA, www.graphpad.com). Morphological analysis was carried out similarly to Elabd et al., 2019.⁶¹ Dataset was assessed for normal distribution by Shapiro-Wilk's test ($p > 0.05$) and visually assessing the normal QQ plot. If normality assumptions were not violated, datasets were analysed with an ordinary one-way ANOVA with Tukey correction to account for multiple comparisons. If normality was violated, data was either transformed to log 10 or using other normalising factors (e.g. BL), or analysed using the non-parametric Kruskal-Wallis test for unpaired samples and using Dunn's test to correct for multiple comparisons. Rate of hatching was analysed with a two-way repeated measures ANOVA with "genotype" and "time" as factors and "subject" as matched set and using Tukey correction to account for multiple comparisons.

Larval behavioural assays and novel tank diving

Corresponding data was analysed using R version 4.0.0 and Rstudio version 1.2.5042 and results of all statistical analyses were reported with respect to a type-1 error rate of $\alpha = 0.05$. Data analysis was performed similarly as previously described³³ but with small changes.

For FLDT, we created three subsets of data to be analysed separately: baseline, light, and dark periods. Baseline period was fitted to the linear mixed model with the total distance travelled as a response variable, genotype as fixed effects, and fish ID as random effects. Light and dark periods constituted the three similar events combined. To explore the change in larvae movement over time in the light (increase) and in the dark (decrease) over time, linear models at light and dark periods were fitted using distance travelled as response variable, interaction between genotype and time as independent variable and fish ID as random effects. Linear mixed models were calculated using R package lme4 and significant fixed effects identified using chi-squared test. To further characterise the effects, where significant differences were established, and post-hoc Tukey test using R package 'multcomp' were carried out. The β coefficient in light and dark period models represents the increase or decrease in distance travelled over time and can be interpreted as the larval 'recovery rate'.

For the flash of light and acoustic startle habituation test, data was divided into 4 parts: baseline period 1, flash of light+recovery, baseline period 2 and response to startle stimuli. Baseline period 1 and 2 were analysed as described above. Response to the flash of light was analysed by looking at total distance moved in 2 seconds following the flash and the rate of recovery. In the "jump" analysis, data was fitted to the linear mixed model with the total distance travelled as a response variable, genotype as fixed effects, and fish ID as random effects. The slope was analysed as previously described in FLD analysis, where the linear model was fitted with distance travelled as response variable, interaction between genotype and time as independent variable and fish ID as random effects.

Response to startle stimuli was analysed in two different ways. In both approaches, each TAP event was defined as a two second event, consisting of exact time of the startle stimuli and the following second. In the first approach, we calculated slope of habituation to startle stimuli by fitting a linear mixed model using distance travelled as response variable, interaction between genotype and tap event as independent variable and fish ID as random effects. Then, significant fixed effects were identified using chi-squared test and, when significant differences were established, post-hoc Tukey test was used to further characterise the effects. In the second approach, we defined a response/non-response status for each fish with threshold for responsive status defined as mean distance moved per second during the basal period plus two standard deviations (SD). The threshold was calculated for all three genotypes together, as genotype was not a significant predictor of basal distance travelled. Each fish was assigned as 'responder' if it moved more than the threshold during the TAP event or as 'non-responder' if it did not. Using the R package 'betareg', we modelled beta regression with percentage of fish responding to stimulus as a response variable and interaction between TAP event number and genotype as explanatory variables. Then, likelihood ratio tests for nested regression models were performed to assess if the interaction between TAP event number and genotype was a significant predictor of individual responsiveness.

In the novel tank diving assay, data on distance travelled in the tank and distance from the bottom of the tank was fitted to a linear mixed model with the total distance travelled and distance from bottom (considering that as the absolute bottom inside the tank) in 30 second bins as a response variable, time and genotype as fixed effects, and fish ID as random effects. To analyse differences in the time spent in the bottom third of the tank, we performed beta regressions using the R package 'betareg'. To analyse genotype differences in the number of transitions between the top and the bottom of the tank, we fitted the data to a generalized linear mixed model with Poisson distribution using the number of transitions to the top-bottom of the tank as response variable, time and genotype as fixed effects, and fish ID as random effects. In all novel tank diving data analyses, the first 30 seconds were excluded as recording of the assay is started prior to the fish being added.

Ontogeny of sociability behaviour

Corresponding data was analysed using GraphPad Prism 9.0.2 for Windows. An ordinary 2-way ANOVA was used to assess genotype \times age interaction of the correlation indexes for each contrast (0 vs. 3 or 0 vs. 1). The differences in SPI each week of testing within genotypes were analysed similarly as Dreosti et al., 2015³⁸: the non-parametric two-tailed Wilcoxon signed-rank test of paired samples. Correlation indexes were analysed with the non-parametric test of Kruskal-Wallis of not paired samples and using Dunn's test to correct for multiple comparisons.